Membrane Fusion in Vesicles of Oligomerizable Lipids

Bart Jan Ravoo, Wilke D. Weringa, and Jan B. F. N. Engberts
Department of Organic and Molecular Inorganic Chemistry and Groningen Biomolecular Sciences and Biotechnology Institute, University of Groningen, 9747 AG Groningen, The Netherlands

ABSTRACT Membrane fusion has been examined in a model system of small unilamellar vesicles of synthetic lipids that can be oligomerized through the lipid headgroups. The oligomerization can be induced either in both bilayer leaflets or in the inner leaflet exclusively. Oligomerization leads to denser lipid headgroup packing, with concomitant reduction of lipid lateral diffusion and membrane permeability. As evidenced by lipid mixing assays, electron microscopy, and light scattering, calcium-induced fusion of the bilayer vesicles is strongly retarded and inhibited by oligomerization. Remarkably, oligomerization of only the inner leaflet of the bilayer is already sufficient to affect fusion. The efficiency of inhibition and retardation of fusion critically depend on the relative amount of oligomeric lipid present, on the concentration of calcium ions, and on temperature. Implications for the mechanism of bilayer membrane fusion are discussed in terms of lipid lateral diffusion and membrane curvature effects.

INTRODUCTION

Membrane fusion is a primordial event in all living organisms. It is the cornerstone of major transmembrane transport processes such as exocytosis and endocytosis and synaptic neurotransmission. Membrane fusion is a key step in cell fertilization and virus infection. Understanding the rules of membrane fusion poses an outstanding challenge to bioscientists, both because of its fundamental relevance to the microbiology of all organisms, and because of its potential involvement in the development of transmembrane transport vehicles for medical purposes, such as drug delivery systems and gene transfection.

Recently, research efforts have focused on the intricate protein machinery that triggers, targets, and controls membrane fusion in living organisms (Rothman, 1996; Hay and Scheller, 1997; Woodman, 1997). Interestingly, it appears that many essential elements in this machinery are conserved from yeast to mammalian cells. Nevertheless, our mechanistic knowledge of in vivo membrane fusion remains far from complete.

As for the molecular rearrangements that occur when two bilayer membranes merge into one, views have converged to a generally accepted model (Siegel, 1993; Chernomordik and Zimmerberg, 1995). Briefly, it is assumed that two adjacent bilayers are brought into close contact, either by anchoring proteins that pull them together (Hughson, 1995), or by fusogenic ions that expel hydration water and eliminate electrostatic repulsion (Papahadjopoulos et al., 1990; Leckband et al., 1993), or by polymer-induced depletion (Lentz, 1994), and that close approximation is accompanied by local disruption of the bilayer structure, leading to the transient establishment of a stalk-like structure. The stalk is believed to expand into a hemifusion intermediate in which the two fusing compartments are separated by one mutual bilayer membrane, the "bilayer diaphragm." Consequently, it is proposed that as the diaphragm widens, a minute hole forms in it, leading to the formation of a fusion pore of limited size. Pore formation is thought to be reversible up to a certain size, beyond which the pore irreversibly opens and full fusion is achieved.

This model of membrane fusion is supported by a large amount of sound data from fluorescence studies and membrane capacitance and conductance measurements of a variety of bilayer membrane systems that clearly demonstrate the sequence of events (Lee and Lentz, 1997), the sensitivity of the kinetics of formation of the various intermediate states to changes in the spontaneous curvature of either of the two bilayer leaflets (Chernomordik et al., 1993; 1995a,b; Melikyan et al., 1997), and the reversibility of hemifusion and pore formation (Nanavati et al., 1992; Lee and Lentz, 1997; Chanturiya et al., 1997).

However, ultrastructural evidence for the model is scarce and scattered. No lipid stalk has ever been unambiguously identified. "Point defects" and "lipidic intramembranous particles," indicative of primary contact sites of adjacent bilayers that may be on the verge of fusion, were observed in freeze-fracture electron microscopy of concentrated lipid suspensions containing substantial amounts of phosphatidylethanolamine (Hui et al., 1981; Verkleij, 1984). Generally, these phenomena are associated with the onset of lamellar-to-inverted hexagonal phase transitions, which have also been identified in cryoelectron microscopy studies of more dilute liposome solutions (Siegel et al., 1989, 1994; Siegel and Epand, 1997; Frederik et al., 1989, 1991). Very recently, structural features of influenza virus-liposome fusion were revealed in freeze-fracture electron microscopy of pelleted virus/liposome mixtures (Kanaseki et al., 1997). Most of the studies mentioned above have suffered from the

Received for publication 8 June 1998 and in final form 21 September 1998.

Address reprint requests to Dr. Jan B. F. N. Engberts, Department of Organic and Molecular Inorganic Chemistry and Groningen Biomolecular Sciences and Biotechnology Institute, University of Groningen, Nijenborgh 4, 9747 AG Groningen, the Netherlands. Tel.: 31-50-3634242; Fax: 31-50-3634296; E-mail: j.b.f.n.engberts@chem.rug.nl.

© 1999 by the Biophysical Society

0006-3495/99/01/374/13 $2.00

inherent transient nature of the fusion event: all intermediate stages of membrane fusion have limited lifetimes, they are localized events that occur infrequently, and observations are essentially a matter of "lucky shots." In many systems this problem has been circumvented by a drastic increase in concentration, making them poor models for biological systems.

In addition, the stalk-pore model of membrane fusion is based on considerations of hydrophobic attractions and curvature stress but does not take electrostatic interactions and (de)hydration effects into account. Therefore, it is not certain that it provides an accurate description of bilayer fusion processes that are induced by calcium ion binding or mediated by proteins.

We report a novel system of liposomes that "fuse in slow motion." We argue that fusion kinetics in liposomes at constant temperature and concentration are principally governed by the ease of lateral diffusion of the lipids in the bilayer and by changes in the spontaneous curvature of either of the two membrane leaflets, and we show that when lipid mobility in the bilayer is restricted and the curvature of the inner leaflet is reduced by means of covalent oligomerization of the lipid headgroups, calcium-induced bilayer fusion proceeds more slowly and less efficiently. It has always been assumed that a decreased fusogenicity of polymerized bilayers explains in part their increased colloidal stability (Fendler, 1984), but we are not aware of any systematic experimental study of the fusion of vesicles of polymerized lipids.

The synthetic lipids used in this study (Scheme 1) differ from naturally abundant phospholipids in the sense that they contain ether instead of ester linkages, and that they carry a β-nitrostyrene (BNS) moiety linked to the phosphate headgroup. The ether linkages make these lipids more robust against pH changes without affecting other membrane properties (Paltauf et al., 1971; Bittman et al., 1984). The main phase transition temperatures of the bilayers are -1°C for DDPBNS, 40°C for DHPBNS, and 54°C for DOPBNS (see Scheme 1). The BNS group is a bifunctional reactive group that can be either hydrolyzed or polymerized. As illustrated in Scheme 1 and described in detail (Ravoo et al., 1996), brief UV irradiation of a vesicle solution of BNS lipids leads to formation of oligomers of at least four or five lipid molecules in both bilayer leaflets. No monomers persist, and we have no indications of lateral heterogeneities in the membrane upon oligomerization (Sackmann et al., 1985). Alternatively, below T_m the BNS units in the outer leaflet of bilayer vesicles can be cleaved efficiently during a pH jump of the external medium, after which the remaining BNS groups in the inner leaflet can be oligomerized by UV irradiation. In this way, vesicles that contain lipid oligomers exclusively in the inner leaflet can be obtained. For the C16 and C18 lipids, the transmembrane asymmetry can be maintained over several days: the half-life of flip-flop for the lipid monomers is 6 and 20 h, respectively (Ravoo et al., 1996), and we assume that the oligomers translocate considerably more slowly. Neither the hydrolytic cleavage nor the oligomerization affects the main phase transition temperature, but the transition becomes less cooperative upon oligomerization (Ravoo et al., 1996).

This paper describes membrane fusion of small unilamellar vesicles (SUVs) with oligomerized lipids in either both leaflets or only the inner bilayer leaflet. By means of a combination of fluorometric, spectroscopic, and microscopic techniques we show that we have developed a dilute system of vesicles in which calcium-induced fusion occurs in "slow motion." Calcium-induced aggregation of the vesicles is not affected. Most interestingly, oligomerization of only the inner bilayer leaflet is sufficient to inhibit membrane fusion. We emphasize that the strict transmembrane asymmetry makes these vesicles fundamentally different from mixed liposomes of fusogenic and nonfusogenic lipids (such as phosphatidylserine and phosphatidylcholine (Düzgünez et al., 1981a,b; Silvius and Gagné, 1984) or phosphatidic acid and phosphatidylcholine (Leventis et al, 1986)). Finally, we discuss the implications of our observations for the mechanism of calcium-induced bilayer fusion, as well as the potential of this system to elucidate intermediate fusion structures.

MATERIALS AND METHODS

Materials

DDPBNS, DHPBNS, DHPPFP, and DOPBNS were synthesized as described (Ravoo et al., 1996). Lipids were stored as 10–20 mM stock solutions in chloroform. Carboxyfluorescein (a mixture of 5- and 6-carboxyfluorescein; Eastman Kodak Co.) and R18 (*n*-octadecyl rhodamine B chloride; Molecular Probes) were generously provided by the Laboratory of Physiological Chemistry of our university.

Scheme 1

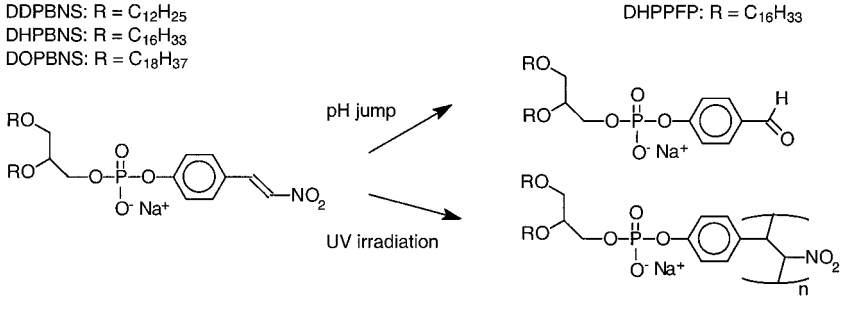

Preparation of unilamellar vesicles

Thin lipid films were prepared from 50–200-μl aliquots of stock solutions in chloroform by rotary evaporation of the solvent. After the addition of buffer (1–5 ml), small unilamellar vesicles were prepared by 20 s of vortexing and 2.5 min/ml sonication at temperatures well above T_m. Sonication was carried out in a Branson Sonifier (Cell Disrupter B15) with an immersion-type microtip operating in pulse mode at 30–40% power output in 30–40% duty cycles. Large unilamellar vesicles were prepared by repeated freeze-thawing of the hydrated lipid film, followed by extrusion through a 200-nm polycarbonate membrane in a LiposoFast Basic extruder (at temperatures above T_m). The procedure for the preparation of vesicles with oligomerized lipids has been reported (Ravoo et al., 1996). For oligomerization of both leaflets, the vesicle solution is irradiated with UV light for 10 min. For oligomerization of only the inner bilayer leaflet, the vesicles are subjected to an external pH jump (25 min at pH 12), which results in hydrolysis of the oligomerizable BNS groups at the outer bilayer leaflet exclusively, followed by 10 min of UV irradiation, leading to oligomerization of the BNS groups in the inner bilayer leaflet only.

Carboxyfluorescein leakage assays

Leakage assays were performed according to literature procedures (Weinstein et al., 1977). Briefly, SUVs were prepared by sonication of 5 mM of the appropriate lipid(s) in a solution of 20 mM carboxyfluorescein (CF) in 5 mM HEPES/NaAc buffer (pH 7.4, 120 mM NaCl). Nonencapsulated CF was removed by rapid filtration over Sephadex G75 at room temperature, using 5 mM HEPES/NaAc buffer (pH 7.4, 140 mM NaCl) as the eluent. Oligomerization of the lipids in the SUVs was carried out immediately after this separation. Leakage at time t was expressed in percentage relative to the initial fluorescence F_0 and the maximum fluorescence F_{TX} obtained after lysis of the SUVs by Triton X-100 (0.5% w/v) according to $(F_t - F_0)/(F_{TX} - F_0) \times 100\%$. Fluorescence was recorded on a SLM-Aminco SPF-500C spectrofluorometer. In all experiments with CF, an excitation wavelength of 490 nm and an emission wavelength of 520 nm were used.

Vesicle solubilization

SUV solubilization by Triton X-100 was measured as the rate of relief of self-quenching of R18 upon disruption of the vesicles by the detergent. SUVs containing 2 mol% of R18 were prepared by sonication and solubilized by 0.5% (w/v) Triton X-100. The initial rate of solubilization was taken from the tangent of the increase of fluorescence versus time and expressed as a percentage of the maximum fluorescence per second. In all experiments with R18, an excitation wavelength of 560 nm and an emission wavelength of 590 nm were used.

R18 fusion assays

Vesicle fusion was monitored using the R18 assay for lipid mixing (Hoekstra et al., 1984). Lipid mixing is recorded as a relief of self-quenching of R18 as it is diluted upon fusion of labeled and unlabeled vesicles. Vesicles (5 μM) with 2% R18 and vesicles (20 μM) without fluorescent label were mixed in 2 ml of 5 mM HEPES/NaAc buffer (pH 7.4, 140 mM NaCl) at the appropriate temperature. The sample was stirred continuously. Fluorescence before the addition of $CaCl_2$ was taken as 0% fusion (F_0), and fusion was initiated by the addition of 0.5–10 mM $CaCl_2$. The extent of mixing (F_{obs}) was measured when the fluorescence increase had stopped and after the addition of four equivalents of EDTA. The value for complete fusion (F_{100}, complete mixing, i.e., 1:5 dilution of R18) was calculated from the fluorescence at infinite dilution (F_{inf}) upon the addition of 0.5% w/v of Triton X-100. F_{obs} and F_{inf} were corrected for volume changes. The extent of fusion for each experiment was calculated as extent (%) = $(F_{obs} - F_0)/0.8(F_{inf} - F_0) \times 100\%$. The initial rate of fusion was calculated from the tangent of the increase of fluorescence versus time and was expressed in percentage of fusion per second. Inhibition of fusion (a decreased extent of fusion) was expressed in percentage relative to a reference experiment according to $(1 - \text{extent}_{obs}/\text{extent}_{ref}) \times 100\%$, and retardation of fusion (a decreased initial rate of fusion) was expressed according to $(1 - \text{rate}_{obs}/\text{rate}_{ref}) \times 100\%$. The results reported in Tables 1 and 2 and Figs. 2, 5, and 6 are the averages of three to five independent experiments. Standard deviations do not exceed 15%, but it was observed that the R18 assay is sensitive to small variations in SUV sonication time and temperature, sample temperature, and concentration.

Carboxyfluorescein leakage during vesicle fusion

Carboxyfluorescein (CF) was entrapped in SUVs of DHPBNS as described above. DHPBNS SUVs (5 μM) containing 20 mM CF and 20 μM DDPBNS SUVs were mixed in 2 ml of 5 mM HEPES/NaAc buffer (pH 7.4, 140 mM NaCl added), and fusion was induced by the addition of 1–5 mM $CaCl_2$. After 5–10 min, calcium ions were removed by the addition of four equivalents of EDTA. Finally, the SUVs were solubilized with Triton X-100. The extent of leakage during fusion was calculated from F_0, the fluorescence before fusion; F_{obs}, the fluorescence observed after addition of $CaCl_2$ and EDTA; and F_{TX}, the fluorescence recorded after detergent solubilization of the SUVs, as described above.

Transmission electron microscopy

Electron micrographs were taken on a Philips EM300 operating at 80 kV. Samples were prepared on formvar/carbon-coated grids exposed to glow discharge and briefly stained with an aqueous PTA solution (2% w/v).

TABLE 1 Extent of fusion of DHPBNS and DOPBNS SUVs*

		endo-oligo-BNS		*endo* + *exo-oligo*-BNS	
$[Ca^{2+}]$ (mM)	*mono*-BNS extent (%)	Extent (%)	Inhibition[#] (%)	Extent (%)	Inhibition[#] (%)
4:1 DHPBNS symmetrical fusion[§]					
1.0	14	0	100	0	100
3.0	35	3.7	89	2.8	92
5.0	45	23	49	21	53
10	56	32	57	28	50
4:1 DHPBNS-DOPBNS (R18) asymmetrical fusion[§]					
1.0	3.7	0	100	0	100
3.0	24	7.7	68	5.5	77
5.0	37	22	41	13	65
10	42	45	−7	33	21
4:1 DOPBNS-DHPBNS (R18) asymmetrical fusion[§]					
1.0	1.3	0	100	0	100
3.0	30	20	33	21	30
5.0	48	42	13	40	17
10	55	55	0	45	18
4:1 DOPBNS symmetrical fusion[§]					
1.0	7.7				
3.0	28				
5.0	42				
10	58				

*Extents of fusion were recorded by the R18 assay for lipid mixing at 50°C (60°C for symmetric DOPBNS SUV fusion).
[#]Inhibitions are expressed relative to the extent of fusion for SUVs before oligomerization.
[§]Total lipid concentration, 25 μM.

TABLE 2 Rate of fusion of DHPBNS and DOPBNS SUVs*

		endo-oligo-BNS		*endo* + *exo-oligo*-BNS	
$[Ca^{2+}]$ (mM)	*mono*-BNS rate (%/s)	Rate (%/s)	Retardation# (%)	Rate (%/s)	Retardation# (%)
4:1 DHPBNS symmetrical fusion§					
3.0	3.0	≪0.1	>95	≪0.1	>95
5.0	7.0	0.54	93	0.19	97
10	17	2.5	85	1.4	92
4:1 DHPBNS-DOPBNS (R18) asymmetrical fusion§					
3.0	0.45	0.17	62	<0.1	>78
5.0	2.0	0.87	56	0.22	89
10	2.7	2.7	0	0.83	69
4:1 DOPBNS-DHPBNS (R18) asymmetrical fusion§					
3.0	2.9	<0.1	>95	<0.1	>95
5.0	7.0	0.53	92	0.37	95
10	15	4.6	69	4.6	69
4:1 DOPBNS symmetrical fusion§					
3.0	1.0				
5.0	3.9				
10	9.4				

*Rates of fusion were recorded by the R18 assay for lipid mixing at 50°C (60°C for symmetrical DOPBNS SUV fusion).
#Retardations are expressed relative to the rate of fusion for SUVs before oligomerization.
§Total lipid concentration 25 μM.

Quasielastic light scattering

Measurements were performed on a Nicomp Model 370 Submicron Particle Sizing System. The values reported are the mean diameters obtained from a number-weighted Gaussian analysis of the scattering data. A volume-weighted analysis yields significantly larger mean diameters (reflecting the small number of LUVs present) but identical trends.

^{31}P NMR

Line widths and relaxation times were measured at 30°C for 20 mM DDPBNS SUVs in 5 mM HEPES/NaAc buffer (pH 7.4) containing 10% D_2O. T_1 was determined by the inversion-recovery method. Spectra were recorded on a Varian 500 MHz machine (with ^{31}P resonance at 202 MHz).

RESULTS

Vesicle solubilization and contents leakage

The initial rate of solubilization (lysis) of SUVs by Triton X-100 was measured as the initial rate of relief of self-quenching of R18 upon the addition of 0.5% (w/v) of the detergent to the SUV solution. R18 fluorescence is low when the probe is present in the bilayer at 2 mol% concentration, and solubilization by Triton X-100 results in a strong increase in fluorescence due to the formation of mixed micelles of Triton X-100 and DHPBNS, in which R18 is diluted to such an extent that self-quenching is completely relieved. The rate at which R18 self-quenching is relieved is a measure of the rate at which the vesicles are solubilized. For DHPBNS (with C16 hydrocarbon chains) an initial rate of 34 ± 4%/s was measured. For SUVs with an oligomerized inner leaflet, an initial rate of 17 ± 3%/s was found, and for SUVs with both leaflets oligomerized, an initial rate of 17 ± 2%/s was found. Thus solubilization is two times slower for the oligomerized bilayer relative to the monomeric bilayer, irrespective of whether only the inner leaflet or both of the bilayer leaflets are oligomerized.

Contents leakage of the SUVs was monitored by measuring the release of trapped CF. Some results are presented in Fig. 1. For DDPBNS, with C12 hydrocarbon chains, it was found that the SUVs are very leaky at room temperature. The half-life of contents release is only 10 min. Upon oligomerization of DDPBNS in both bilayer leaflets of the vesicles, they retain their contents much longer: for oligomerized DDPBNS, the half-life of release is 60 min. However, it should be noted that CF acts as a strong UV filter, and oligomerization is much less efficient in its presence. Up to 30% of the lipid remains in its monomeric form. The addition of 25 mol% of cholesterol to the vesicles leads to an increased half-life of release of 50 min. This is a well-known effect: above T_m, cholesterol condenses the hydrophobic interior and reduces the permeability of the bilayer (Bittman et al., 1984). Apparently, oligomerization has a comparable effect on contents release.

Compared to DDPBNS, SUVs of DHPBNS (with C16 hydrocarbon chains) are nonleaky. At room temperature, less than 3% of trapped CF is lost from the vesicles after 2 days, irrespective of whether the lipids have been oligomerized. At 50°C, however, well above T_m, SUVs of DHPBNS are permeable to CF. Without oligomerization, most of the trapped CF is released within 15 min. If both bilayer leaflets are oligomerized, the bilayer is much less permeable. The half-life of contents release is more than 2 h. If only the inner bilayer leaflet is oligomerized, the SUVs are only slightly more permeable.

^{31}P NMR and lipid headgroup mobility

Phosphorus-31 NMR spectra of SUVs of DDPBNS (with C12 hydrocarbon chains) yielded insight into the effect of oligomerization on the headgroup mobility of the lipids in the bilayer. Before oligomerization, the spectrum shows one isotropic signal with a line width of ~30 Hz and a relaxation time T_1 of 0.5 s. This is indicative of fast tumbling SUVs with rapid lipid lateral diffusion (Cullis, 1976; Burnell et al., 1980). After oligomerization, a line width of ~230 Hz and an unchanged T_1 of 0.5 s were found. Because we can exclude slower tumbling of oligomerized SUVs relative to monomeric SUVs because no significant change of vesicle diameter was observed upon oligomerization (vide infra), we interpret the increased line width as an indication of slower lateral diffusion of the lipid oligomers in the bilayer. However, a contributing line-broadening effect due to chemical shift differences between the various oligomers cannot be ruled out. Although the relaxation time T_1 is indifferent to lipid oligomerization, a change in lipid

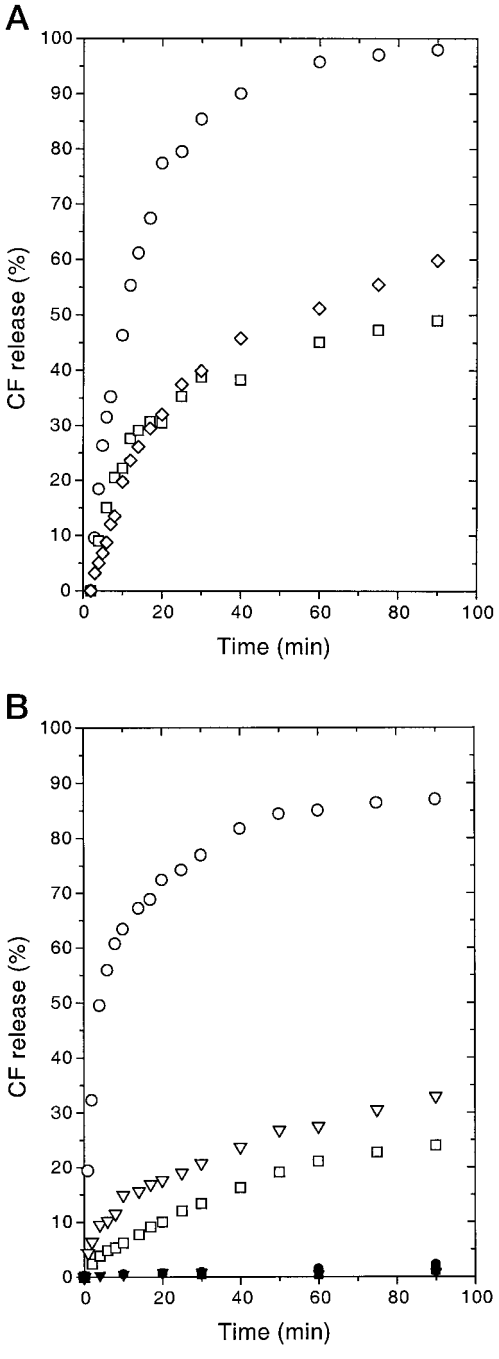

FIGURE 1 (*A*) Release of encapsulated carboxyfluorescein from SUVs of DDPBNS at 25°C. ○, DDPBNS; ◇, DDPBNS with 25 mol% cholesterol; □, oligomerized DDPBNS. (*B*) Release of encapsulated carboxyfluorescein from SUVs of DHPBNS at 25°C (●, ■, ▼) and at 50°C (○, □, ▽). ○, ●, DHPBNS; ▽, ▼, DHPBNS with oligomerized inner leaflet; □, ■, DHPBNS with both leaflets oligomerized.

headgroup mobility cannot be excluded solely on this ground. Interpretation of T_1 values in bilayer systems is often ambiguous (Smith and Ekiel, 1984).

Calcium-induced vesicle fusion

Vesicle fusion was induced by the addition of 0.5–10 mM $CaCl_2$. The process was monitored by lipid mixing assays, transmission electron microscopy, and quasielastic light scattering. Lipid mixing was measured by the R18 assay (Hoekstra et al., 1984). Although it is known that the R18 assay disagrees with other fusion assays under certain circumstances (Stegmann et al., 1993, 1995), we were unable to use the resonance energy transfer (RET) assay employing rhodamine and *N*-7-nitrobenz-2-oxa-1,3-diazol-4-yl-amino (NBD)-labeled phosphatidylethanolamine (Struck et al., 1981) or assays employing pyrene (Pal et al., 1988), because the BNS moiety inhibits efficient NBD or pyrene excitation, through either quenching or absorbance in the excitation wavelength range. However, we established that the R18 and the RET assay yield identical results for calcium-induced fusion of SUVs of DHPPFP (which does not interfere with NBD excitation), and therefore the R18 assay was employed with confidence. Moreover, in all experiments it was carefully verified that no probe exchange occurred spontaneously, and no probe dilution was observed in the absence of unlabeled vesicles.

An overview of the extent of fusion of the BNS lipid SUVs as recorded by the R18 assay is presented in Fig. 2. The assay was carried out at 50°C, except for the experiment with DOPBNS, which was done at 60°C. All lipid vesicles fuse quite efficiently and rapidly. The increase of fluorescence stopped after 1–5 min (depending on the calcium ion concentration), indicating completion of the fusion process within that period. The threshold calcium ion concentration for fusion is 0.5 mM. The highest extents and rates of fusion are reached at 5 mM calcium ion. At higher calcium ion concentrations, flocculation of fusion products

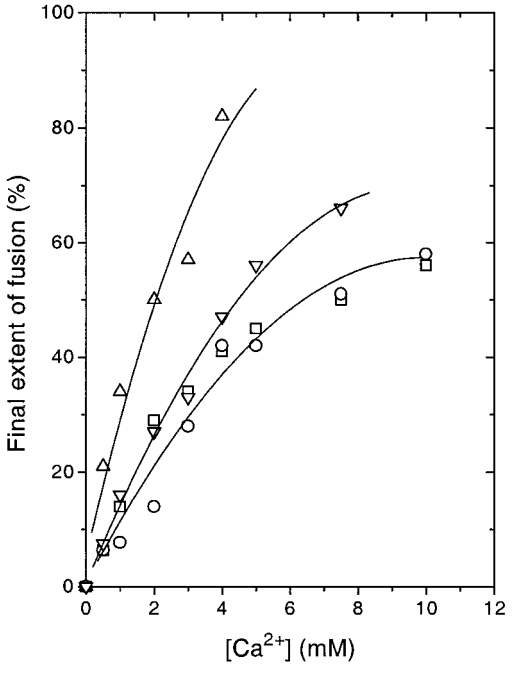

FIGURE 2 Calcium-ion concentration dependence of the extent of symmetrical fusion of SUVs of DDPBNS (△), DHPBNS (□), DOPBNS (○), and DHPPFP (▽). Extents of fusion were recorded by the R18 assay for lipid mixing at 50°C (60°C for DOPBNS).

becomes a dominant process. Short-chain lipid SUVs fuse more efficiently than long-chain lipid SUVs (DDPBNS > DHPBNS > DOPBNS). Cleavage of the BNS moiety has a marginal effect on the extent of SUV fusion (DHPBNS versus DHPPFP). It was observed that no significant fusion occurs below T_m of the bilayers.

Vesicle fusion was examined in more detail for SUVs of DHPBNS at 50°C (Tables 1 and 2). The extent of fusion is dependent on the calcium ion concentration: fusion is negligible below 0.5 mM calcium ion, it increases with calcium ion concentration up to 5 mM, and it levels off at higher calcium ion concentrations. Fusion is strongly inhibited by oligomerization of the lipids in the SUVs. No fusion occurs below 3 mM calcium ion. Interestingly, the inhibition is comparable for SUVs in which both bilayer leaflets are oligomerized and SUVs in which only the inner bilayer leaflet is oligomerized. The relative efficiency of inhibition is dependent on the calcium ion concentration: it is optimal (> 90%) up to 3 mM and decreases to 50% at higher calcium ion concentrations. Similar observations were made for the rate of fusion. Representative values of the rate of lipid mixing upon the addition of $CaCl_2$ are reported in Table 2. The fusion process is fastest at the highest calcium ion concentrations and is strongly retarded by oligomerization of the bilayer. It took up to 20 min for the increase of fluorescence to stop, indicating completion of the fusion process. The retardation of fusion is more than 95% at low calcium ion concentration and only slightly less at higher calcium ion concentrations. Furthermore, the data indicate that fusion proceeds slower in SUVs in which both bilayer leaflets are oligomerized than in SUVs in which only the inner bilayer is oligomerized. Comparable results were obtained for SUVs of DDPBNS (Ravoo et al., manuscript submitted for publication).

Because it is known that small and large vesicles can show different fusion behaviors (see, e.g., Nir et al., 1982), fusion of LUVs was tested in a control experiment. Compared to that of SUVs, the extent of fusion of 200 nm LUVs was slightly higher (max. 20% higher at 10 mM calcium ion), but the rate of fusion was much lower (max. 80%). However, upon oligomerization of both bilayer leaflets, inhibition and retardation of fusion were quantitatively similar to the effect observed in SUV fusion. We contend that SUVs and LUVs respond identically to lipid oligomerization.

The results from the lipid mixing assays were confirmed by transmission electron microscopy of negatively stained SUVs before and after fusion. Fig. 3 is a representative collection of micrographs. It shows the disappearance of most SUVs and the large overall increase in vesicle diameter that occurs upon induction of fusion of DHPBNS SUVs (Fig. 3, *A* and *B*). In contrast, extensive aggregation of SUVs but relatively little fusion are found for DHPBNS SUVs in which both bilayer leaflets have been oligomerized (Fig. 3 *C*). Similar results are found for DDPBNS (Ravoo et al., manuscript submitted for publication).

Quasielastic light scattering provided the average changes in vesicle diameter during the fusion process. Fig. 4 shows data obtained from scattering experiments. All vesicle solutions are rather polydisperse, particularly after fusion. These findings correspond well with the results obtained with TEM. For a sample of DDPBNS (Fig. 4 *A*),

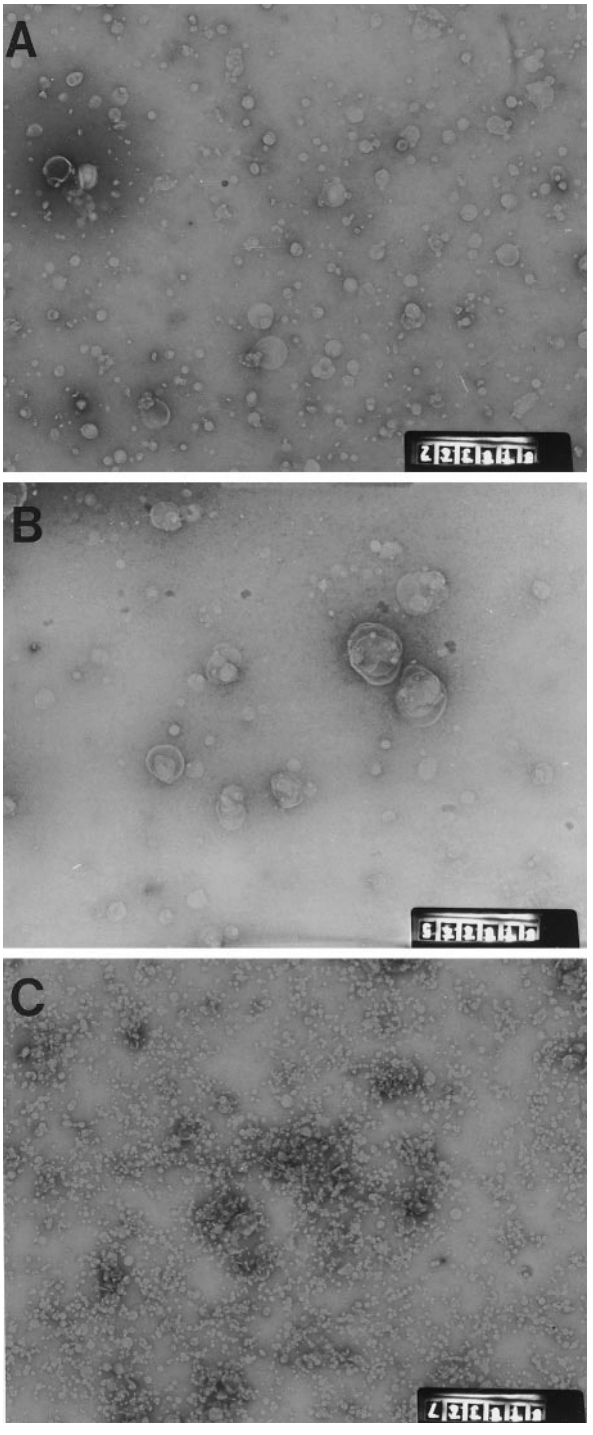

FIGURE 3 Electron micrographs of SUVs of DHPBNS stained with PTA. (*A*) SUVs of DHPBNS. (*B*) LUVs of DHPBNS that result from fusion of the SUVs after the addition of 5 mM $CaCl_2$, 2 min incubation at 50°C, and the addition of four equivalents of EDTA. (*C*) Persistence of SUVs of oligomerized DHPBNS after the addition of 5 mM $CaCl_2$ at 50°C. Magnification 20,000×, 1 cm = 500 nm.

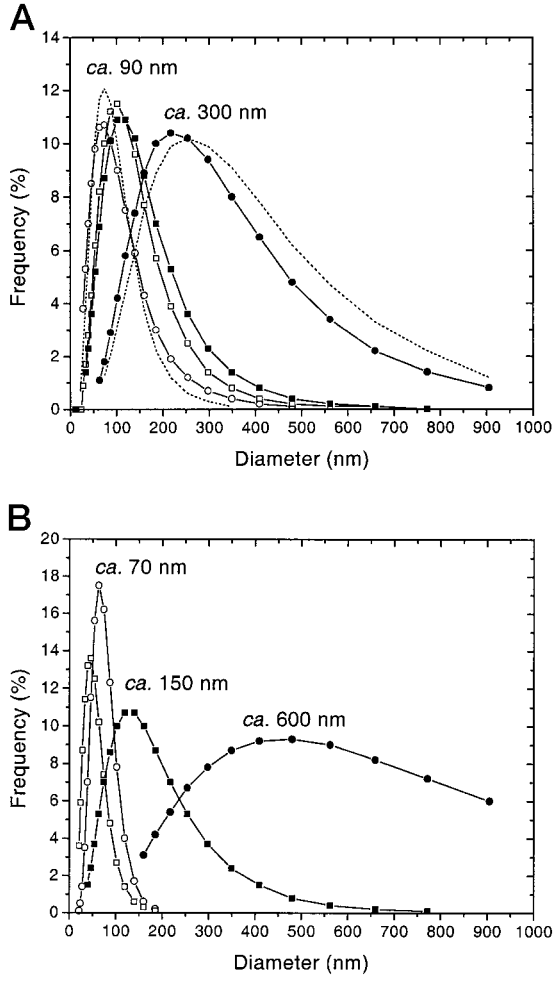

FIGURE 4 (*A*) Number-weighted size distribution of vesicles of DDPBNS (○, ●) and oligomerized DDPBNS (□, ■) before (○, □) and after (●, ■) fusion. Fusion was induced at 25°C by the addition of 5 mM $CaCl_2$ (removed after 10 min by four equivalents of EDTA). The dashed lines represent the size distributions that result from fusion at 45°C. (*B*) Number-weighted size distribution of vesicles of DHPBNS (○, ●) and oligomerized DHPBNS (□, ■) before (○, □) and after (●, ■) fusion. Fusion was induced at 45°C by the addition of 5 mM $CaCl_2$ (removed after 10 min by four equivalents of EDTA).

the mean diameter before fusion was 90 nm. Upon the addition of 5 mM $CaCl_2$ at room temperature, the diameter increased more than fourfold, indicating extensive aggregation and fusion of the SUVs. A stable, reproducible value was not reached; instead, the fusion and aggregation process was quenched by the addition of EDTA. The mean diameter after fusion is 300 nm, a threefold increase, which means that on average, ~10 SUVs fused into one large unilamellar vesicle (LUV). For a sample of oligomerized DDPBNS with a mean diameter before fusion of 90 nm, again a large increase was found upon the addition of $CaCl_2$, indicating extensive aggregation of SUVs. However, upon the addition of EDTA a mean diameter of 110 nm was found, an increase of only 20%, which means that the SUVs of oligomerized DDPBNS aggregate but hardly fuse at all. At 45°C, the experiment gave identical results. For a sample of DHPBNS at 45°C (Fig. 4 *B*), the number-weighted diameter was 70 nm before fusion and ~600 nm after fusion. After oligomerization of the lipids, induction of fusion only resulted in an increase in diameter to 150 nm, indicative of strongly inhibited fusion compared to the monomer lipid SUVs.

Asymmetrical vesicle fusion

In addition to the symmetrical vesicle fusion experiments described above, several asymmetrical fusion experiments were monitored with the R18 assay. In these experiments, SUVs of DHPBNS (with C16 hydrocarbon chains and T_m = 40°C) were targeted at SUVs of DOPBNS (with C18 hydrocarbon chains and T_m = 54°C) and vice versa. Because the experiments were carried out at 50°C, SUVs of DOPBNS have a gel-like bilayer ($T < T_m$), and no symmetrical fusion can take place. SUVs of DHPBNS have a liquid-crystalline bilayer ($T > T_m$), and fusion occurs readily—both symmetrically and asymmetrically—but symmetrical fusion is not reported by the assay, because it does not result in R18 dilution.

Extents and rates of asymmetrical fusion are presented in Tables 1 and 2. Results are described for fusion of SUVs of DOPBNS, labeled with R18, with four equivalents of SUVs of DHPBNS (so that the assay reports dilution of R18 in target DOPBNS vesicles due to fusion with DHPBNS vesicles) and for fusion of SUVs of DHPBNS, labeled with R18, with four equivalents of SUVs of DOPBNS (so that the assay reports dilution of R18 in target DHPBNS vesicles due to fusion with DOPBNS vesicles). In either case it was observed that the extent and rate of fusion increase with calcium ion concentration. Below 1.0 mM no fusion is observed, and whereas the maximum extent of fusion is reached at 5 mM calcium ion (and levels off at higher concentrations), the rate of fusion is highest at the highest calcium ion concentration. The final extents of fusion are comparable to those observed in the symmetrical fusion experiments. The observed rates of fusion are very different for the two asymmetrical experiments. For DHPBNS targeted at DOPBNS slow fusion is observed, with rates even smaller than those found for symmetrical DOPBNS SUV fusion, most likely because of competition from symmetrical fusion of DHPBNS SUVs. For DOPBNS targeted at DHPBNS much faster fusion is observed that is comparable to symmetrical DHPBNS SUV fusion. Thus in either case the target membrane composition is rate determining.

Upon oligomerization of the lipids in the DHPBNS SUVs (and not in the DOPBNS SUVs), lipid mixing is inhibited and retarded, and the fusion threshold concentration of calcium ion increases to ~2 mM. If both bilayer leaflets of the DHPBNS SUVs are oligomerized, considerable inhibition (up to 75%) and retardation (60–75%) are observed when DHPBNS is targeted at DOPBNS, and modest inhibition (max. 30%) but strong retardation (75–95%) are observed when DOPBNS is targeted at DHPBNS. If only the inner bilayer leaflet of the DHPBNS SUVs is oligomer-

ized, considerable inhibition (max. 70%) is observed when DHPBNS is targeted at DOPBNS, but only modest inhibition (max. 30%) is observed when DOPBNS is targeted at DHPBNS. Concerning the rates of fusion, modest retardation (max. 50%) is observed when DHPBNS is targeted at DOPBNS, but strong retardation (80–95%) is found when DOPBNS is targeted at DHPBNS. In all fusion experiments, the inhibitory and retarding effects of oligomerization decrease with increasing calcium ion concentration. Both inhibition and retardation are more pronounced when DHPBNS is targeted at DOPBNS than vice versa, and they are clearly less pronounced in the asymmetrical experiments compared to the symmetrical fusion experiments.

The temperature dependence of the extent of fusion of DHPBNS targeted at DOPBNS is presented in Fig. 5. As anticipated, the extent of fusion for the monomeric DHPBNS SUVs follows a sigma profile with a sharp increase around 40°C, which corresponds to the T_m of DHPBNS. Below 40°C, fusion activity is very low, and slightly above T_m the maximum extent of fusion is reached. No additional increase is found above 54°C, which is the T_m of DOPBNS. Upon oligomerization of both bilayers in DHPBNS SUVs, fusion is considerably inhibited. Around T_m of DHPBNS, a gradual increase of the extent of fusion sets in. Above T_m of DOPBNS, a significant additional increase of fusion is observed. The trend indicates that at high temperature, monomeric and oligomerized DHPBNS SUVs fuse equally efficiently with DOPBNS SUVs. This implies that the optimal temperature window for the inhibition of fusion is between the T_m's of DHPBNS and DOPBNS.

In a second set of asymmetrical fusion experiments, SUVs of DDPBNS (with C12 hydrocarbon chains and $T_m = -1$°C) were targeted at SUVs of DHPBNS (with C16 hydrocarbon chains and $T_m = 40$°C). To monitor both lipid mixing and contents leakage in the course of fusion, vesicles of DHPBNS were either labeled with R18 or loaded with CF. The experiments were carried out at 25°C, i.e., above T_m of DDPBNS, but below T_m of DHPBNS. It was carefully verified that under these conditions, no spontaneous lipid mixing or CF leakage occurs. Therefore, any R18 or CF dilution must result from asymmetrical fusion of the DHPBNS vesicles with the DDPBNS vesicles. The results are presented in Fig. 6. From the R18 assay it is evident that SUVs of DDPBNS targeted at SUVs of DHPBNS fuse efficiently. No significant leakage of CF is observed upon the addition of calcium ion, indicating an essentially nonleaky fusion process. The 1:5 dilution of contents that results from complete fusion does not lead to measurable relief of CF self-quenching. However, we found that CF is rapidly released after the addition of EDTA, that is, after quenching of the fusion process and after break-up of the aggregated clusters of fused SUVs. We conclude that leakage during fusion is limited, but leakage from the mixed LUVs that result from fusion is significant. This is consistent with the finding that DHPBNS SUVs are impermeable to CF, whereas DDPBNS SUVs are very leaky (vide supra),

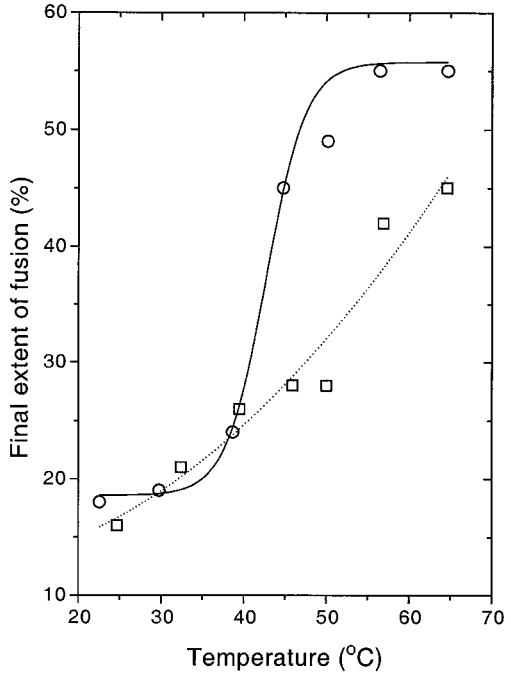

FIGURE 5 Temperature dependence of the extent of asymmetrical fusion of SUVs of DHPBNS (○) and SUVs of oligomerized DHPBNS (□) targeted at SUVs of DOPBNS. Extents of fusion were recorded by the R18 assay for lipid mixing.

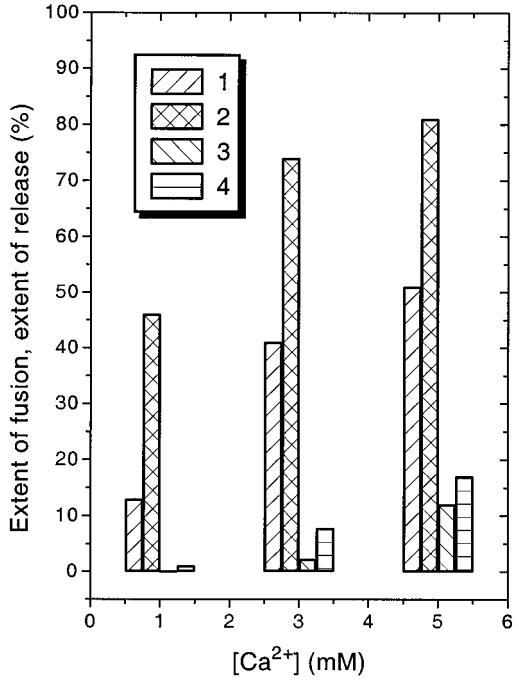

FIGURE 6 Comparison of the calcium ion concentration dependence of the extent of lipid mixing and the release of encapsulated carboxyfluorescein as a result of fusion of SUVs of DDPBNS targeted at SUVs of DHPBNS at 25°C. Extents of lipid mixing before and after oligomerization are given in lanes 1 and 3, respectively. Extents of contents release before and after oligomerization are given in lanes 2 and 4, respectively.

and with available literature data indicating that calcium-induced liposome fusion can occur with retention of aqueous contents (Wilschut et al., 1983; Hui et al., 1988). Furthermore, CF leakage is secondary to lipid and contents mixing in calcium-induced fusion of phosphatidylserine liposomes (Wilschut et al., 1980). When SUVs of oligomerized DDPBNS were targeted at SUVs of oligomerized DHPBNS, only low extents of lipid mixing and contents release were observed. As expected, the target SUVs retain their contents in the absence of fusion. Again, in all experiments the extent of lipid mixing and contents release increases with calcium ion concentration, but the inhibition due to oligomerization decreases.

Effects of EDTA addition

In all experiments using the R18 assay for lipid mixing, the observed extent of fusion as reported in Table 1 and Figs. 2 and 6 was determined when the fluorescence had reached its maximum, and after removal of calcium ion by the addition of four equivalents of EDTA. In the experiments with monomer lipid SUVs, the addition of EDTA resulted in an instantaneous decrease in fluorescence. We attribute this decrease to a break-up of vesicle aggregates and to a decrease in turbidity and scattering in the sample, with concomitant decrease in the recorded fluorescence. In line with this explanation, the effect was most significant at the highest calcium ion concentrations (up to 30%), but very small at low calcium ion concentrations. In contrast, in the experiments with oligomerized lipid vesicles (either in both leaflets or only in the inner leaflet), the addition of EDTA resulted in an increase in fluorescence. This suggests further lipid mixing upon removal of calcium ion. The increase amounted to up to 25% and increased with calcium ion concentration but decreased with temperature.

In addition to this, we note that calcium ion binding causes domain formation in bilayer membranes of anionic lipids (Hoekstra, 1982; Haverstick and Glaser, 1987; Papahadjopoulos et al., 1990; Leckband et al., 1993), which is relieved upon removal of calcium ion by EDTA. We propose that the same process occurs in bilayers of lipids with BNS headgroups. This is supported by the observation that at subfusion threshold concentrations of calcium ion, and even in the absence of unlabeled SUVs (so that no R18 dilution can occur), the addition of calcium ions results in a minor decrease in fluorescence (domain formation, clustering of R18, increased self-quenching), which is relieved upon the addition of EDTA (removal of calcium ion, homogenization of the bilayer, relief of self-quenching).

DISCUSSION

Lipid mobility in oligomerized bilayers

When all present results are taken together, a consistent picture emerges of the properties of SUVs of oligomerized lipids. Compared to their monomer lipid counterparts, the oligomerized vesicles are less permeable and more resistant to detergent solubilization. Oligomerization may be considered a mild form of polymerization, for which similar results have often been described (Singh and Schnur, 1993). Permeability and detergent solubilization are affected to an equally large extent when either both or only the inner bilayer leaflet is oligomerized. For the contents leakage assay this might be as anticipated, because it is the inner bilayer leaflet that poses the primary barrier for outward permeation. As for the solubilization experiments, we suggest that the process of bilayer swelling due to uptake of detergent, which is considered to be the first step in solubilization by nonionic detergents (Kragh-Hansen et al., 1993), proceeds less readily in oligomerized bilayers than in monomeric bilayers, irrespective of whether the oligomers are present in both bilayer leaflets or only in the inner one.

Reduced permeability and higher detergent resistance suggest a denser packing of the headgroups, and indeed, comparison of ^{31}P-NMR and differential scanning microcalorimetric (DSC) data (Ravoo et al., 1996) indicates that the oligomerization reaction results in a more rigid packing of the headgroups of the lipid molecules in the bilayer, without affecting the flexibility of the hydrocarbon chains in the bilayer interior. Thus the main effect of oligomerization is a reduced mobility of the headgroups in an otherwise fluid bilayer. This implies a reduction of the lateral diffusion of the lipid molecules. At 202 MHz, we measured an eightfold increase in the ^{31}P line width upon oligomerization. For comparison, a fivefold decrease in the ^{31}P line width (at 129 MHz) was reported for SUVs of dipalmitoylphosphatidylcholine upon a temperature increase from 30°C to 50°C, i.e., below and above the T_m (McLaughlin et al., 1975). By means of a viscosity dependence study of the line width, this decrease in line width was correlated with a 20-fold increase in the lateral diffusion coefficient of the lipid molecules (Cullis, 1976). These NMR data strongly suggest that oligomerization results in a drastic decrease in lateral diffusion. Furthermore, our findings are corroborated by results from computer simulations of bilayers of lipids with polymerizable headgroups (Pink et al., 1993), which indicate that even when present in small amounts (less than 10 mol%), short, linear lipid polymers (20 monomers per polymer) have a lateral diffusion coefficient that is at least two orders of magnitude smaller than that of the monomers. Using the technique of fluorescence recovery after photo bleaching, Sackmann (Sackmann et al., 1985) measured a 70% decrease in the overall lateral diffusion coefficient in bilayers of a lipid with polymerized headgroups. In this case, the degree of polymerization was estimated to be ~100, and the polymer concentration was only 0.5 mol% (50 mol% monomer and complete polymerization). In our case, although the degree of polymerization is lower, the concentration of oligomer is much higher (~100 mol%), and a drastic decrease in the lateral diffusion coefficient was anticipated.

Fusion of oligomerized lipid bilayer membranes

Oligomerization of the lipid molecules does not influence calcium-induced aggregation but strongly affects bilayer fusion of vesicles of BNS lipids. Lipid mixing and contents release assays, electron microscopy, and quasielastic light scattering yield consistent results. Under fusogenic conditions, oligomerized vesicles aggregate but retain their contents and do not grow in size. Lipid mixing is inhibited up to 10-fold in its extent, and it proceeds more than 10 times more slowly. In all of the experiments described above, the inhibitions are less pronounced than the retardations. Therefore we conclude that the oligomerization has an influence on the kinetics rather than on the extent of bilayer fusion. In absolute terms, lipid mixing during calcium-induced fusion of SUVs of BNS lipids is a matter of 1–5 min, depending on temperature and calcium ion concentration. These rates are normal for calcium-induced vesicle fusion (Wilschut et al., 1980; Düzgünez et al., 1981a,b; Nir et al., 1982; Silvius and Gagné, 1984; Leventis et al., 1986) and comparable to the rates recently reported for poly(ethylene glycol)-induced fusion (Lee and Lentz, 1997) and biological membrane fusion (Lee and Lentz, 1997). However, upon oligomerization of the lipids, fusion proceeds much more slowly and takes up to 20 min to arrive at much lower final extents. Oligomerized lipid membranes "fuse in slow motion."

It is important to note that the inhibitions that are reported by the R18 assay are undoubtedly inhibitions of lipid mixing as a result of fusion and not inhibitions of the assay as a result of slower lateral diffusion of the probe in the oligomerized membrane. Assuming a lateral diffusion coefficient of 1 $\mu m^2/s$ for the lipid monomers, and a 20-fold reduction upon oligomerization, it can be calculated that scrambling of the oligomers over the surface of the small vesicles occurs on a time scale of seconds, whereas slow fusion requires up to 20 min.

Remarkably, the inhibition and retardation of fusion are similar for vesicles in which both the outer and the inner bilayer leaflets or only the inner bilayer leaflet is oligomerized. The additional inhibiting and/or retarding effect of oligomerization of the lipids in the outer bilayer leaflet is almost negligible. In accordance with previous observations, it is the composition of the inner rather than the outer bilayer leaflet that controls the completion of bilayer fusion (Chernomordik et al., 1995a,b; Melikyan et al., 1997).

The effect of lipid oligomerization on vesicle fusion is dependent on three parameters. First, the effect is more pronounced when more of the membranes participating are oligomerized, e.g., compare symmetrical fusion experiments (in which two oligomerized membranes fuse) and asymmetrical fusion experiments (in which only one of two fusing membranes is oligomerized). Alternatively, one could state that the effect of lipid oligomerization is stronger at a higher relative oligomer content of the membranes in fusion, irrespective of the location of the oligomerized lipids. This observation matches the results from studies using mixed liposomes composed of fusogenic phosphatidylserine or phosphatidic acid and nonfusogenic phosphatidylcholine (Düzgünez et al., 1981a,b; Silvius and Gagné, 1984; Leventis et al., 1986), in which fusion is progressively slower as the phosphatidylcholine contents are increased. Second, we found a decreasing effect of oligomerization at higher calcium ion concentration. We suggest that when more calcium ion is present, more fusion contact sites can be established and fusion is more rapid. This is consistent with the notion that calcium-induced vesicle fusion is normally aggregation-rate limited (Wilschut et al., 1980; Nir et al., 1980) but becomes fusion-rate limited at high calcium ion concentration and reduced fusion rate. Finally, we have observed that the effect of lipid oligomerization decreases with temperature. As will be discussed below, this is consistent with the concept of oligomerized lipids posing a kinetic barrier to fusion.

Implications for the mechanism of bilayer fusion

Membrane fusion is a localized event in which two adjacent membranes approach, establish a microscopic region of "molecular contact," bend into sharply curved transient structures, and eventually merge into one continuous membrane. This process demands flexibility of the membrane, which is largely governed by 1) the thermotropic state of the hydrocarbon interior, 2) the lateral diffusion coefficient of the lipid molecules, and 3) the spontaneous curvature of the membrane leaflets.

As for the hydrocarbon interior, it is well known that below the main phase transition temperature of the membrane, when the interior is in the gel-like lamellar state, fusion activity is low if not absent (Wilschut et al., 1985). The hydrocarbon interior has a rigid packing, lipids diffuse only very slowly across and over the bilayer, and the membrane is stiff compared to the fluid state above T_m. However, according to our DSC data, the influence of oligomerization of the lipids on the thermotropic phase behavior of the hydrocarbon interior is modest and cannot be invoked to explain the strong inhibition and retardation of fusion observed upon oligomerization.

We contend that a high lateral diffusion coefficient of the lipid molecules in the membrane is a prerequisite for efficient membrane fusion. The molecular rearrangement of the lipid bilayers in the course of fusion will only take place at an appreciable rate if the lipid molecules have sufficient degrees of freedom. In this report we have demonstrated that oligomerization of the lipid headgroups results in a large reduction of the lateral diffusion rate. If both the inner and the outer bilayer leaflets are oligomerized, fusion is most likely inhibited, because the membrane will resist formation of membrane defects that would otherwise result in stalk-like fusion sites (vide infra). If only the inner bilayer leaflet is oligomerized, stalks may be formed, but fusion pore formation is expected to be very slow. The observation that inhibition and retardation of fusion increase with a higher oligomer content of the membranes undergoing fu-

sion, irrespective of the location of the oligomers, is entirely consistent with the fact that the lateral diffusion coefficient decreases with an increasing oligomer content (Pink et al., 1993; Sackmann et al., 1985). Furthermore, the observation that inhibition and retardation of fusion decrease with temperature is also consistent with the notion of a decreased lateral diffusion of the oligomerized lipids: at higher temperatures, lateral diffusion is faster, and the effects of lipid oligomerization diminish.

Concerning the spontaneous curvature of the bilayer, it is known that hemifusion is inhibited by lipids with a positive curvature (which tend to form micelles) in the outer membrane leaflet, because they disfavor formation of stalk-like fusion sites with negative curvature (Chernomordik et al., 1995a,b). In some cases, lipids with negative curvature (which tend to form inverted phases) have a modest promoting effect (Chernomordik et al., 1995a,b). In contrast, fusion pore formation and full fusion benefit from the presence of lipids with a positive curvature in the inner bilayer leaflet, whereas lipids with a negative curvature have a strongly inhibiting effect (Chernomordik et al., 1995a,b; Melikyan et al., 1997). Our data suggest that the headgroups of the BNS lipids pack closer upon oligomerization, which would promote increased negative curvature of the oligomerized bilayer leaflet (compare Sackmann et al., 1985, 1986; Srisiri et al., 1997). Thus pore formation and full fusion would be strongly inhibited if the inner bilayer leaflet were oligomerized. This implies that hemifusion can occur, but full fusion is inhibited. In terms of bilayer spontaneous curvature, oligomerization of the outer membrane leaflet may have only a small effect on the membrane fusion process (Chernomordik et al., 1995a,b).

So far it is not clear what the role of calcium ion is in the stages of the fusion process beyond the establishment of a region of molecular membrane contact. It is assumed that calcium-induced bilayer fusion is triggered by changes in lateral compressibility and structural defects that result from binding of calcium ion to negatively charged lipid headgroups (Papahadjopoulos et al., 1990). Complexation of calcium ion yields an essentially anhydrous calcium ion-lipid complex, but electrostatic interactions and (de)hydration effects are not taken into account at all in the stalk-pore hypothesis of membrane fusion (Siegel, 1993; Chernomordik and Zimmerberg, 1995). Nevertheless, analogous models have been proposed for calcium-induced membrane fusion (Papahadjopoulos et al., 1990). One could imagine that structural defects as well as phase transitions are kinetically suppressed in bilayers of oligomerized bilayers and that this poses an additional barrier to calcium-induced bilayer fusion. Similarly, it is anticipated that defects and phase transitions occur more readily in bilayers of lipids with short hydrocarbon chains than in bilayers of lipids with long hydrocarbon chains, which may explain why the former fuse more readily.

We speculate that the observation of further lipid mixing upon removal of calcium ion from the oligomerized SUVs is an indication of a collapse of hemifused structures into full fusion. It is known that binding of calcium ions to anionic lipid headgroups leads to denser headgroup packing as a result of a reduction of electrostatic and hydration repulsions and interlipid binding. Denser headgroup packing leads to increased negative curvature, resulting in calcium-induced lamellar-to-inverted hexagonal phase transitions in bilayers containing phosphatidic acid or cardiolipin (Cullis and de Kruijff, 1979; Verkleij et al., 1982; Hong et al., 1988). However, this is not a general phenomenon, because calcium ion does not generate inverted hexagonal phases with phosphatidylserine, despite strong promotion of fusion (Papahadjopoulos et al., 1975). It is possible that the presence of calcium ions is a prerequisite not only for stalk formation, but also for the persistence of negatively curved hemifusion intermediates, which either relapse into unfused vesicles or collapse into full fusion upon the removal of calcium ions by EDTA.

We contend that a "slow motion fusion" system has been devised that may allow fusion intermediate structures to be studied by ultrastructural techniques. As demonstrated, lipid oligomerization leads to a reduced rate and extent of calcium-induced vesicle fusion. In the case of vesicles with an oligomerized inner bilayer leaflet only, we anticipate that highly curved stalk and hemifusion intermediates may form readily, but completion of fusion is strongly inhibited. Further work along these lines is currently in progress.

The authors express their gratitude to Prof. A. D. R. Brisson and Mr. J. F. L. van Breemen for the hospitality of the Electron Microscopy Department, and to Prof. D. Hoekstra for discussion of the results and for the hospitality of the Laboratory of Physiological Chemistry.

REFERENCES

Bittman, R., S. Clejan, S. Lund-Katz, and M. C. Phillips. 1984. Influence of cholesterol on bilayers of ester- and ether-linked phospholipids. *Biochim. Biophys. Acta.* 772:117–126.

Burnell, E. E., P. R. Cullis, and B. de Kruijff. 1980. Effects of tumbling and lateral diffusion on phosphatidylcholine model membrane ^{31}P NMR line shapes. *Biochim. Biophys. Acta.* 603:63–69.

Chanturiya, A., L. V. Chernomordik, and J. Zimmerberg. 1997. Flickering fusion pores comparable with initial exocytotic pores occur in protein-free phospholipid bilayers. *Proc. Natl. Acad. Sci. USA.* 94: 14423–14428.

Chernomordik, L. V., A. Chanturiya, J. Green, and J. Zimmerberg. 1995a. The hemifusion intermediate and its conversion to complete fusion: regulation by membrane composition. *Biophys. J.* 69:922–929.

Chernomordik, L. V., M. M. Kozlov, and J. Zimmerberg. 1995b. Lipids in biological membrane fusion. *J. Membr. Biol.* 146:1–14.

Chernomordik, L. V., S. S. Vogel, A. Sokoloff, H. O. Onaran, E. A. Leikina, and J. Zimmerberg. 1993. Lysolipids reversibly inhibit Ca^{2+}-, GTP-, and pH-dependent fusion of biological membranes. *FEBS Lett.* 318:71–76.

Chernomordik, L. V., and J. Zimmerberg. 1995. Bending membranes to the task: structural intermediates in bilayer fusion. *Curr. Opin. Struct. Biol.* 5:541–547.

Cullis, P. R. 1976. Lateral diffusion rates of phosphatidylcholine in vesicle membranes: effects of cholesterol and hydrocarbon phase transitions. *FEBS Lett.* 70:223–228.

Cullis, P. R., and B. de Kruijff. 1979. Lipid polymorphism and the functional roles of lipids in biological membranes. *Biochim. Biophys. Acta.* 559:399–420.

Düzgünez, N., S. Nir, J. Wilschut, J. Bentz, C. Newton, A. Portis, and D. Papahadjopoulos. 1981a. Calcium and magnesium-induced fusion of mixed phophatidylserine/phosphatidylcholine vesicles: effect of ion binding. *J. Membr. Biol.* 59:115–125.

Düzgünez, N., J. Wilschut, R. Fraley, and D. Papahadjopoulos. 1981b. Studies on the mechanism of membrane fusion. Role of head group composition in calcium and magnesium-induced fusion of mixed phospholipid vesicles. *Biochim. Biophys. Acta.* 642:182–195.

Fendler, J. H. 1984. Polymerized surfactant vesicles: novel membrane mimetic agents. *Science.* 223:890–894.

Frederik, P. M., K. N. Burger, M. C. A. Stuart, and A. J. Verkleij. 1991. Lipid polymorphism as observed by cryo-electron microscopy. *Biochim. Biophys. Acta.* 1062:133–141.

Frederik, P. M., M. C. A. Stuart, and A. J. Verkleij. 1989. Intermediary structures during membrane fusion as observed by cryo-electron microscopy. *Biochim. Biophys. Acta.* 979:275–278.

Haverstick, D. M., and M. Glaser. 1987. Visualization of Ca^{2+}-induced phospholipid domains. *Proc. Natl. Acad. Sci. USA.* 84:4475–4479.

Hay, J. C., and R. H. Scheller. 1997. SNAREs and NSF in targeted membrane fusion. *Curr. Opin. Cell Biol.* 9:505–512.

Hoekstra, D. 1982. Fluorescence method for measuring the kinetics of Ca^{2+}-induced phase separations in phosphatidylserine-containing lipid vesicles. *Biochemistry.* 21:1055–1061.

Hoekstra, D., T. de Boer, K. Klappe, and J. Wilschut. 1984. Fluorescence method for measuring the kinetics of fusion between biological membranes. *Biochemistry.* 23:5675–5681.

Hong, K., P. A. Baldwin, T. M. Allen, and D. Papahadjopoulos. 1988. Fluorometric detection of the bilayer-to-hexagonal phase transition in liposomes. *Biochemistry.* 27:3947–3955.

Hughson, F. M. 1995. Molecular mechanisms of protein-mediated membrane fusion. *Curr. Opin. Struct. Biol.* 5:507–513.

Hui, S. W., S. Nir, T. P. Stewart, L. T. Boni, and S. K. Huang. 1988. Kinetic measurements of fusion of phosphatidylserine containing vesicles by electron microscopy and fluorometry. *Biochim. Biophys. Acta.* 941:130–140.

Hui, S. W., T. P. Stewart, and L. T. Boni. 1981. Membrane fusion through point defects in bilayers. *Science.* 212:921–923.

Kanaseki, T., K. Kawasaki, M. Murata, Y. Ikeuchi, and S. Ohnishi. 1997. Structural features of membrane fusion between influenza virus and liposome as revealed by quick-freezing electron microscopy. *J. Cell Biol.* 137:1041–1056.

Kragh-Hansen, U., M. LeMaire, J. P. Noël, T. Gulik-Krzywicki, and J. V. Møller. 1993. Transitional steps in the solubilization of protein-containing membranes and liposomes by nonionic detergent. *Biochemistry.* 32:1648–1656.

Leckband, D. E., C. A. Helm, and J. Israelachvili. 1993. Role of calcium in the adhesion and fusion of bilayers. *Biochemistry.* 32:1127–1140.

Lee, J., and B. R. Lentz. 1997. Evolution of lipidic structures during model membrane fusion and the relation of this process to cell membrane fusion. *Biochemistry.* 36:6251–6259.

Lentz, B. R. 1994. Polymer-induced membrane fusion: potential mechanism and relation to cell fusion events. *Chem. Phys. Lipids.* 73:91–106.

Leventis, R., J. Gagné, N. Fuller, R. P. Rand, and J. R. Silvius. 1986. Divalent cation induced fusion and lipid lateral segregation in phosphatidylcholine-phosphatidic acid vesicles. *Biochemistry.* 25:6978–6987.

McLaughlin, A. C., P. R. Cullis, J. A. Berden, and R. E. Richards. 1975. ^{31}P NMR of phospholipid membranes: effects of chemical shift anisotropy at high magnetic field strengths. *J. Magn. Res.* 20:146–165.

Melikyan, G. B., S. A. Brener, D. C. Ok, and F. S. Cohen. 1997. Inner but not outer membrane leaflets control the transition from glycosylphosphatidylinositol-anchored influenza hemagglutinin-induced hemifusion to full fusion. *J. Cell Biol.* 136:995–1005.

Nanavati, C., V. S. Markin, A. F. Oberhauser, and J. M. Fernandez. 1992. The exocytotic fusion pore modeled as a lipidic pore. *Biophys. J.* 63:1118–1132.

Nir, S., J. Bentz, and J. Wilschut. 1980. Mass action kinetics of phosphatidylserine vesicle fusion as monitored by coalescence of internal vesicle volumes. *Biochemistry.* 19:6030–6036.

Nir, S., J. Wilschut, and J. Bentz. 1982. The rate of fusion of phospholipid vesicles and the role of bilayer curvature. *Biochim. Biophys. Acta.* 688:275–278.

Pal, Y., Y. Barenholz, and R. R. Wagner. 1988. Pyrene phospholipid as a biological fluorescent probe for studying the fusion of virus membrane with liposomes. *Biochemistry.* 27:30–36.

Paltauf, F., H. Hauser, and M. C. Phillips. 1971. Monolayer characteristics of some 1,2-diacyl, 1-alkyl-2-acyl and 1,2-dialkyl phospholipids at the air-water interface. *Biochim. Biophys. Acta.* 249:539–547.

Papahadjopoulos, D., S. Nir, and N. Düzgünez. 1990. Molecular mechanisms of calcium-induced membrane fusion. *J. Bioenerg. Biomembr.* 22:157–179.

Papahadjopoulos, D., W. J. Vail, K. Jacobson, and G. Poste. 1975. Cochleate lipid cylinders: formation by fusion of unilamellar lipid vesicles. *Biochim. Biophys. Acta.* 394:483–491.

Pink, D. A., R. Merkel, B. Quinn, E. Sackmann, and J. Pencer. 1993. Intersecting polymers in lipid bilayers: cliques, static order parameters and lateral diffusion. *Biochim. Biophys. Acta.* 1150:189–198.

Ravoo, B. J., W. D. Weringa, and J. B. F. N. Engberts. 1996. Design and characterization of synthetic bilayer vesicles with a polymerized inner bilayer leaflet. *Langmuir.* 12:5773–5780.

Rothman, J. E. 1996. The protein machinery of vesicle budding and fusion. *Protein Sci.* 5:185–194.

Sackmann, E., H. P. Duwe, and H. Engelhardt. 1986. Membrane binding elasticity and its role for shape fluctuations and shape transformations of cells and vesicles. *Faraday Discuss. Chem. Soc.* 81:281–290.

Sackmann, E., P. Eggl, C. Fahn, H. Bader, H. Ringsdorf, and M. Schollmeier. 1985. Compound membranes of linearly polymerized and cross-linked macrolipids: preparation, microstructure and applications. *Ber. Bunsenges. Phys. Chem.* 89:1198–1208.

Siegel, D. P. 1993. Energetics of intermediates in membrane fusion: comparison of stalk and inverted micellar intermediate mechanisms. *Biophys. J.* 65:2124–2140.

Siegel, D. P., J. L. Burns, M. H. Chestnut, and Y. Talmon. 1989. Intermediates in membrane fusion and bilayer/nonbilayer phase transitions imaged by time-resolved cryo-transmission electron microscopy. *Biophys. J.* 56:161–169.

Siegel, D. P., and R. M. Epand. 1997. The mechanism of lamellar-to-inverted hexagonal phase transitions in phosphatidylethanolamine: implications for membrane fusion mechanisms. *Biophys. J.* 73:3089–3111.

Siegel, D. P., W. J. Green, and Y. Talmon. 1994. The mechanism of lamellar-to-inverted-hexagonal phase transitions: a study using temperature-jump cryo-electron microscopy. *Biophys. J.* 66:402–414.

Silvius, J. R., and J. Gagné. 1984. Calcium-induced fusion and lateral phase separations in phosphatidylcholine/phosphatidylserine vesicles. Correlation by calorimetric and fusion measurements. *Biochemistry.* 23:3241–3247.

Singh, A., and J. M. Schnur. 1993. Polymerizable phospholipids. *In* Phospholipids Handbook. G. Cevc, editor. Marcel Dekker, New York. 233–291.

Smith, I. C. P., and I. H. Ekiel. 1984. Phosphorus-31 NMR of phospholipids in membranes. *In* Phosphorus-31 NMR, Principles and Applications. D. G. Gorenstein, editor. Academic Press, Orlando, FL. 447–475.

Srisiri, W., T. M. Sisson, D. F. O'Brien, K. M. McGrath, Y. Han, and S. M. Gruner. 1997. Polymerization of the inverted hexagonal phase. *J. Am. Chem. Soc.* 119:4866–4873.

Stegmann, T., J. G. Orsel, J. D. Jamieson, and P. J. Padfield. 1995. Limitations of the octadecylrhodamine dequenching assay for membrane fusion. *Biochem. J.* 307:875–876.

Stegmann, T., P. Schoen, R. Bron, J. Wey, I. Bartoldus, A. Ortiz, J. L. Nieva, and J. Wilschut. 1993. Evaluation of viral membrane fusion assays. Comparison of the octadecylrhodamine assay with the pyrene eximer assay. *Biochemistry.* 32:11330–11337.

Struck, D. K., D. Hoekstra, and R. E. Pagano. 1981. Use of resonance energy transfer to monitor membrane fusion. *Biochemistry.* 20: 4093–4099.

Verkleij, A. J. 1984. Lipidic intramembranous particles. *Biochim. Biophys. Acta.* 779:43–63.

Verkleij, A. J., R. de Maagd, J. Leunissen-Bijvelt, and B. de Kruiff. 1982. Divalent cations and chlorpromazine can induce non-bilayer structures

in phosphatidic acid-containing model membranes. *Biochim. Biophys. Acta.* 684:255–262.

Weinstein, J. N., S. Yoshikami, P. Henkart, R. Blumenthal, and W. A. Hagins. 1977. Liposome-cell interaction: transfer and intracellular release of a trapped fluorescent marker. *Science.* 195:489–492.

Wilschut, J., N. Düzgünes, R. Fraley, and D. Papahadjopoulos. 1980. Studies on the mechanism of membrane fusion: kinetics of calcium ion induced fusion of phosphatidylserine vesicles followed by a new assay for mixing of aqueous vesicle contents. *Biochemistry.* 19:6011–6021.

Wilschut, J., N. Düzgünez, D. Hoekstra, and D. Papahadjopoulos. 1985. Modulation of membrane fusion by membrane fluidity: temperature dependence of divalent cation induced fusion of phosphatidylserine vesicles. *Biochemistry.* 24:8–14.

Wilschut, J., N. Düzgünez, K. Hong, D. Hoekstra, and D. Papahadjopoulos. 1983. Retention of aqueous contents during divalent cation-induced fusion of phospholipid vesicles. *Biochim. Biophys. Acta.* 734:309–318.

Woodman, P. G. 1997. The roles of NSF, SNAPs and SNAREs during membrane fusion. *Biochim. Biophys. Acta.* 1357:155–172.